An Electronegativity-Induced Spin Repulsion Effect

András Stirling*,† and Alfredo Pasquarello‡,§

Computational Science, Department of Chemistry and Applied Biosciences, ETH Zurich, USI Campus, Via Giuseppe Buffi 13, CH-6900 Lugano, Switzerland, Ecole Polytechnique Fédérale de Lausanne (EPFL), Institute of Theoretical Physics, CH-1015 Lausanne, Switzerland, and Institut Romand de Recherche Numérique en Physique des Matériaux (IRRMA), CH-1015 Lausanne, Switzerland

Received: June 21, 2005

We present a spin delocalization effect in radical Si-containing systems, featuring a heteroatom of high electronegativity (such as N, O, or Cl) bonded to the unsaturated Si atom. We find that the higher the electronegativity of the heteroatom, the more the localized spin shifts *away* from the unsaturated Si atom and the heteroatom toward saturated Si neighbors. We demonstrate that this *spin repulsion* toward saturated Si atoms is induced by the electronegativity difference between the Si atom and the heteroatoms. We present a simple molecular-orbital-based mechanism which fully explains the structural and electronic effects. We contrast the present spin delocalization mechanism with the classical hyperconjugation in organic chemistry. The most important consequences of this spin redistribution are the electron-spin-resonance activity of the saturated Si neighbors and the enhanced stability of the radical centers. We predict a similar effect for Ge radicals and discuss why organic systems based on carbon do not feature such spin repulsion.

Introduction

Spin centers in silicon systems are found in a large variety of materials of great technological importance, such as semiconductors, insulators, and silyl radicals. A detailed understanding of the properties of these centers is important, because the occurrence of unpaired electrons often severely undermines the material properties. For instance, unpaired electrons are known to give rise to an enhanced reactivity in chemical processes, which may result in a higher degradability of the material. In Si-based electronic devices, Si dangling-bond defects not only affect the transport properties leading to reduced electrical performance but are also suspected to play a role in the incipience of breakdown phenomena. The experimental characterization of these centers relies to a large extent on their activity in electron-spin-resonance spectroscopy. Modeling approaches based on density functional calculations have proved invaluable in indentifying the underlying structural and electronic properties of these centers through comparisons between calculated and measured hyperfine parameters.[1,2]

The electron-spin-resonance spectrum of the S center in amorphous SiO_2 is characterized by the appearance of two hyperfine doublets.[3] This specific signature has been determinant in the theoretical assignment of the atomic structure of this defect.[1] The center corresponds to a dangling bond mostly localized on a trivalent silicon atom which features an oxygen vacancy in its first-neighbor shell. The theoretical modeling revealed that the spin density in this center is delocalized over the Si−Si bond, and it was suggested that the large electronegativity of the oxygen atoms bonded to the unsaturated Si atoms could trigger this phenomenon.

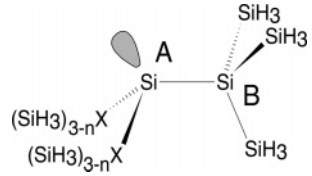

Figure 1. Structure of the clusters used in this work. The Si atom carrying the dangling bond (A) and its saturated Si neighbor (B) are indicated.

In the present study, this spin-delocalization effect and its underlying electronic mechanism are investigated in a systematic way. We performed ab initio calculations on a set of Si clusters all featuring an unsaturated Si atom but with varying first-neighbor atoms taken from the first and second row (H, C, N, O, F, Si, P, S, and Cl). The clusters are illustrated in Figure 1 and can be characterized by the general formula $(X(SiH_3)_{3-n})_2$ $\dot{S}iSi(SiH_3)_3$, where n goes from 0 to 3 as the atom X goes from C (Si) to F (Cl or H) and where $\dot{S}i$ symbolizes the unsaturated Si atom. We investigated the structural and electronic properties of the clusters as a function of the electronegativity carried by the atom X. We describe in detail the mechanism responsible for the displacement of spin density toward the saturated Si atom and demonstrate that the extent of delocalization strongly correlates with the electronegativity of the substituting heteroatoms.

Computational Aspects

The electronic structure calculations were performed within the Kohn−Sham density functional formalism based on the hybrid B3LYP functional.[4] The calculations on the clusters were performed using the *Gaussian 98* and *Gaussian 03* program packages.[8] To accurately describe hyperfine properties, we used basis sets that were specifically designed for calculating magnetic properties. The EPR-III basis set[5] was used for the elements H, C, N, O, and F, whereas the IGLO-III basis set[6,7]

* E-mail: stirling@chemres.hu. Present address: Chemical Research Center, P.O. Box 17, Budapest, Hungary H-1525.
† ETH Zurich.
‡ Ecole Polytechnique Fédérale de Lausanne (EPFL).
§ Institut Romand de Recherche Numérique en Physique des Matériaux (IRRMA).

10.1021/jp053335h CCC: $30.25
Published on Web 08/27/2005

TABLE 1: Hyperfine Contact Interactions (in Gauss) Calculated for Selected Molecules and Compared to Experimental Values Taken from Ref 16[a]

molecule	X	EN	nn	theory	expt
$((CH_3)_3Si)_3\dot{S}i$	Si	1.90	Si	54	64
$(CH_3)_3SiSi(CH_3)_2$	C	2.55	Si	129	137
$CH_3\dot{S}iH_2$	H	2.20	C	178	182
$CH_3\dot{S}iCl_2$	Cl	3.16	C	307	295

[a]For each molecule, we also specify the heteroatom X and its Pauling electronegativity (EN) and the species of the neighboring saturated atom (Si or C).

was employed for the heavier elements Si, P, S, and Cl. After completely relaxing all the structural degrees of freedom, we studied the spin distribution in the clusters through the Mulliken spin densities on the atoms and the isotropic hyperfine interactions (Fermi contact interactions). While the latter quantities can be directly related to experimental observables, the former ones are arbitrarily defined but nevertheless serve for identifying trends.

The Fermi contact interaction is a simple function of the spin density at the nucleus position

$$a = \frac{8\pi}{3} g_e \mu_e g_{Si} \mu_{Si} \rho_s(\mathbf{R}) \tag{1}$$

Here $\rho_s(\mathbf{R}) = \rho_\uparrow(\mathbf{R}) - \rho_\downarrow(\mathbf{R})$ is the electron spin density at the nucleus site $\mathbf{R}$, g_e the free electron g factor, μ_e the Bohr magneton, g_{Si} the nuclear gyromagnetic ratio for Si, and μ_{Si} the corresponding nuclear magneton. Note, that although μ_{Si} assumes negative values, here we chose to reverse the sign of the calculated hyperfine interactions, since only their absolute values are accessible experimentally. Hence, negative hyperfine interactions calculated in the present work indicate excess minority spin density. To verify the accuracy of our method, we have calculated the hyperfine contact interaction of the unsaturated Si atom in a set of molecules with Si−Si and Si−C back-bonds and different X heteroatoms (H, C, Si, Cl) where experimental values are available. Table 1 shows a very nice agreement between theory and experiment irrespective of the chemical environment of the unsaturated Si atom.

The Mulliken spin density of an atom I can be given as

$$\rho_s(\mathrm{I}) = \sum_{\nu \in \mathrm{I}} [(\mathbf{P}^\alpha - \mathbf{P}^\beta)\mathbf{S}]_{\nu\nu} \tag{2}$$

where $\mathbf{P}^s$ is the density matrix composed of the coefficients $C_{\mu i}$ of the linear expansion of the molecular orbitals in terms of the basis functions $\varphi_\mu(\mathbf{r})$

$$\mathbf{P}^s_{\nu\mu} = \sum_{i=1}^{N_s} C^*_{\mu i} C_{\nu i} \tag{3}$$

and $\mathbf{S}$ the overlap matrix

$$\mathbf{S}_{\mu\nu} = \int \varphi^*_\mu(\mathbf{r}) \varphi_\nu(\mathbf{r})\, \mathrm{d}\mathbf{r} \tag{4}$$

The indices μ and ν run over the functions φ_μ in the basis set. In eq 2, the index ν runs over the basis functions localized on the considered atom, while N_s is the number of occupied orbitals in the manifold of spin s.

It has been showed that, within the density functional framework adopted in this work, delocalized electron states are often erroneously preferred to the localized states when close in energy.[9−11] This phenomenon is due to the improper treatment of the self-interaction in the exchange-correlation functional. It has been shown that the sole inclusion of the exact exchange contribution into the energy functional as in the present hybrid scheme does not always suffice to achieve the correct localized states.[10] On the other hand, when the electron correlation is completely neglected as in the pure Hartree−Fock (HF) scheme, the localization is favored in an excessive way. As the structural configurations around the spin centers are highly asymmetric in our systems, we do not expect nearly degenerate states nor artificial delocalization in our systems. Nevertheless, we often compared results obtained within the hybrid density functional scheme with corresponding Hartree−Fock results without noticing important differences as far as the degree of localization of the electronic states is concerned.

TABLE 2: Bond Lengths and Bond Angles of the Unsaturated Si Atom for Varying Heteroatoms X in the Clusters[a]

X	$\dot{S}i-X$ (Å)	$\dot{S}i-Si$ (Å)	$\angle X-\dot{S}i-X$
H	1.487	2.334	112.2°
C	1.917	2.391	117.0°
N	1.753	2.379	112.6°
O	1.643	2.383	108.8°
F	1.611	2.392	107.5°
Si	2.352	2.352	116.7°
P	2.265	2.361	116.8°
S	2.168	2.366	109.5°
Cl	2.091	2.371	108.8°

[a] The indicated angles correspond to the average over the three bond angles.

TABLE 3: Electronic Properties of the Clusters[a]

X	EN	3s	3p	ρ_A	ρ_B	ρ_X	a_A	a_B
H	2.20	27	69	0.938	0.026	0.004	147	6.4
C	2.55	35	62	0.971	−0.010	−0.060	149	17
N	3.04	33	60	0.753	0.088	0.033	192	44
O	3.44	36	61	0.705	0.161	0.036	227	58
F	3.98	40	57	0.715	0.202	0.023	245	52
Si	1.90	26	73	0.976	−0.040	−0.040	82	−3
P	2.19	26	68	0.875	0.003	−0.007	119	10
S	2.58	34	62	0.683	0.078	0.095	191	26
Cl	3.16	44	52	0.674	0.145	0.073	244	34

[a]Pauling electronegativity (EN), relative s and p contribution (in %) in the dangling-bond orbital, spin densities (in atomic units) on the unsaturated Si atom (ρ_A) and on the neighboring saturated Si atom (ρ_B), and corresponding hyperfine contact interactions a_A and a_B (in gauss). The spin densities on the heteroatoms X (ρ_X) are also provided.

Results and Discussion

The principal structural parameters of the optimized clusters are given in Table 2. From the average bond angle on the unsaturated Si atom, one deduces that the radical centers always show a pyramidal structure. For both the second- and third-row heteroatoms, the pyramidalization increases with atomic number. The Si−X distances monotonically decrease with atomic number within a row, while the corresponding Si−Si bonds increase. The only exception to this systematic behavior is observed for C heteroatoms and should be attributed to the steric interaction between the large number of terminating silyl groups present in this case.

The decreasing Si−X bond lengths can simply be interpreted in terms of the decreasing atomic radii of the heteroatoms. However, the other structural variations cannot be explained in such a trivial way and require the consideration of the electronic properties. Table 3 collects the most important electronic properties associated to the set of considered clusters. In Figures 2, 3 and 4, we show the variations of the relevant spin densities

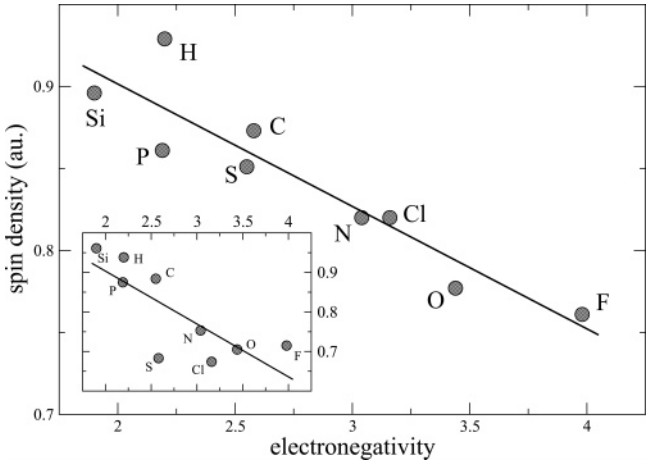

Figure 2. Sum of the spin densities localized on the unsaturated Si atom and on its neighboring heteroatoms vs the electronegativity of the heteroatoms. Inset: the spin density on the unsaturated Si atom alone. The lines are guides to the eyes.

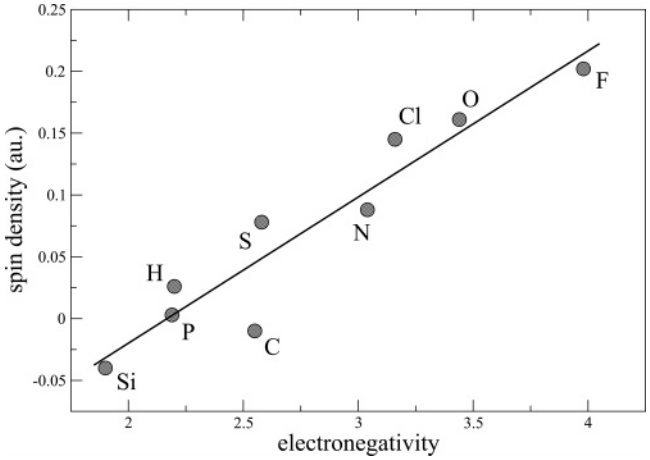

Figure 3. Spin density on the neighboring saturated Si atom vs the electronegativity of the heteroatoms. The line is a guide to the eyes.

and hyperfine interactions as a function of the electronegativity of the heteroatoms.

The first important observation is that, as the electronegativity of the heteroatom increases, the sum of the spin densities localized on the unsaturated atom and on the heteroatom decreases (Figure 2). The same property also holds for the spin density on the unsaturated atom alone, although the observed trend shows somewhat more scattering (Figure 2, inset). These trends are at variance with simple electronegativity considerations, which would suggest electronic attraction toward the heteroatom regardless of spin. Figure 3 shows that the missing spin is accumulating on the neighboring saturated Si atom, for which the spin density is found to increase with the electronegativity of the heteroatom. In other words, electronegative atoms induce spin delocalization toward farther atoms, giving rise to a virtual *spin repulsion*.

The second interesting observation concerns the hyperfine contact interactions, which are found to increase with the electronegativity of the heteroatoms for both the unsaturated Si atom and its saturated neighbor. While the increase of the contact interaction on the saturated Si atom is consistent with the increase of its spin density (Figure 3), opposite trends are observed for the contact interaction and the spin density in the case of the unsaturated silicon. This apparent contradiction can be rationalized by recalling that the contact interaction is only sensitive to s-wave components of the wave functions (cf. eq

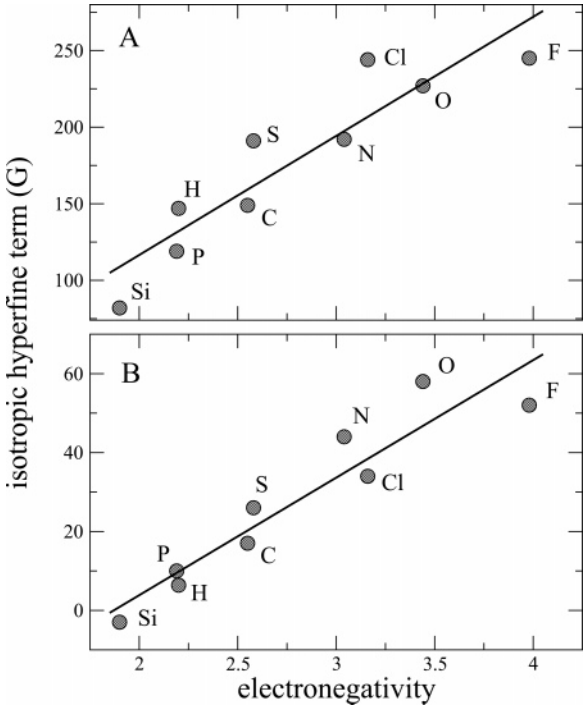

Figure 4. Hyperfine contact interaction for the unsaturated Si atom (A) and for the neighboring saturated Si atom (B) vs the electronegativity of the heteroatoms. The lines are guides to the eyes.

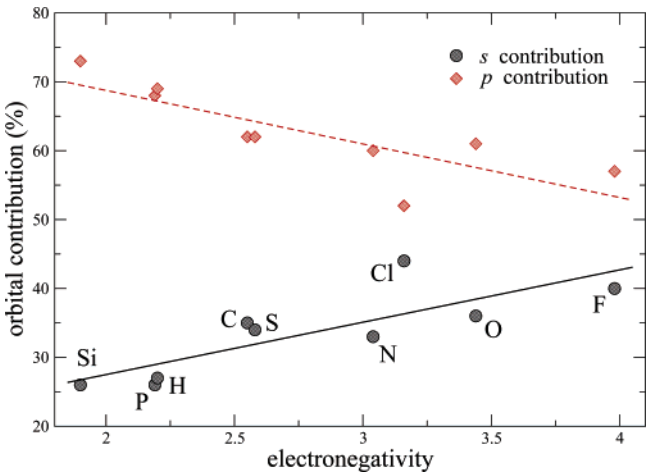

Figure 5. Contribution of the 3*s* and 3*p* orbitals of the unsaturated Si atom to the singly occupied molecular orbital. The lines are guides to the eyes.

1) while the spin density defined here corresponds to the full spin density localized on the atom, irrespective of angular symmetries.

The behavior of the hyperfine contact interaction on the unsaturated Si atom can be understood in terms of the hybridization state of the dangling-bond orbital in the clusters, i.e., the singly occupied molecular orbital (SOMO). In Figure 5, we display the relative contribution from the 3s and 3p valence orbitals of the unsaturated Si atom versus the electronegativity of the heteroatoms. For increasing electronegativity, we find that the p character decreases in favor of the s character, as expected from the behavior of the hyperfine interactions. Therefore, the hybrid state of the unpaired orbital gradually changes from the original sp^3 to a state that is closer to sp^2. This trend is easily explained: the higher the electronegativity of the heteroatoms, the higher the p contribution of the unsaturated Si atom to their bonding orbitals,[12−14] and conse-

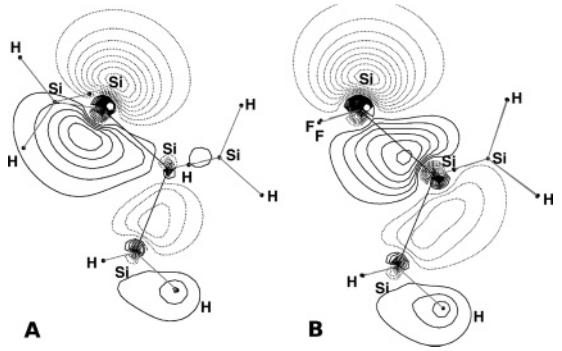

Figure 6. Contour plot of the singly occupied molecular orbitals for the clusters with (A) X = Si and (B) X = F. The orbitals are plotted in the plane defined by the Si_A-Si_B bond and the axis of the dangling bond (identified through the antiperiplanar Si atom). Contour values are indicated by strides of 0.02 atomic units.

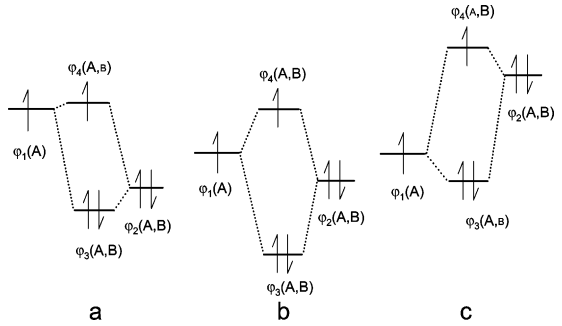

Figure 7. Orbital interaction mechanism responsible for the spin delocalization. φ_1(A) indicates the initial unpaired orbital and φ_2(A,B) the initial bonding orbital between atoms A and B. φ_3(A,B) and φ_4-(A,B) correspond to delocalized orbitals resulting from the interaction between φ_1(A) and φ_2(A,B). The size of the letters provides information concerning the delocalization, the atom indicated by a larger letter carrying more spin density. Three cases are considered: (a) weak interaction, typically with X = Si; (b) large interaction with heteratoms X of high electronegativity; (c) strong spin transfer for highly elongated Si_A-Si_B back-bonds.

quently, the higher the s character in the dangling-bond orbital. The degree of s character in the dangling-bond orbital also reflects in the pyramidality of the bonding of the unsaturated Si atom (Table 2).

The spin density decrease on Si_A and concurrent increase on Si_B cannot directly be understood on the basis of a change in the hybridization state of the dangling-bond orbital. To identify the underlying mechanism, we compare in Figure 6 the singly occupied molecular orbitals corresponding to the clusters with X = Si and X = F. We notice that considerable spin density not only occurs on the unsaturated Si atom but also appears in the region between the silicon atoms A and B. This effect is more pronounced in the case of F heteroatoms and points to an interaction between the Si−Si bond and the unpaired electron. We interpret this behavior following the lines of ref 1 in which a mechanism was outlined for accounting for the spin delocalization at the $\dot{S}i{\equiv}SiO_2$ defect center in amorphous SiO_2. The invoked mechanism is illustrated through an energy diagram involving the interaction between the dangling bond and the back-bond between atoms Si_A and Si_B (Figure 7). Figure 7a corresponds to an unsaturated Si atom that only counts Si atoms among its neighbors (X = Si). In this case, the overlap between the dangling-bond orbital and the Si−Si back-bonds is not favorable because of the large energy difference, and the spin delocalization is minimal. When one or two of the Si neighbors are replaced by atoms of higher electronegativity, the s character of the dangling-bond orbital is enhanced (Figure 5). Because the energy of the 3s level is lower than that of the 3p one, the energy of the dangling bond shifts downward favoring the interaction between the dangling bond and the Si−Si back-bond (Figure 7b). This interaction leads to two molecular orbitals that are delocalized over the Si−Si back-bond. The larger the electronegativity of the X atoms is, the lower the dangling bond energy level is, and thus, the stronger the overlap between the two orbitals. The stabilization that is achieved by this mechanism is analogous to that in the frontier orbital theory,[15] with the HOMO/SOMO interaction replacing the HOMO/LUMO one.

The mechanism described above allows us to rationalize the observations that had not found explanation so far. A higher electronegativity of the heteroatoms causes an enhanced mixing between the dangling-bond orbital and bonding Si−Si orbital. In particular, the resulting singly occupied molecular orbital extends over the full Si−Si back-bond, causing a reduction of the spin density on the unsaturated Si atom (Figure 2) and concurrently bringing spin density to the neighboring saturated Si atom (Figure 3). The hyperfine contact interaction on the latter Si atom is consistently found to increase. The invoked interaction is not expected to affect in a significant way the s-wave contribution of the unsaturated Si atom to the singly occupied molecular orbital. The explanation given above for the increase of its hyperfine contact interaction therefore maintains its validity. Furthermore, the invoked delocalization allows us to understand the observed elongation of the Si−Si back-bond with increasing electronegativity of the heteroatoms (Table 2). Indeed, the original σ-bond between the two Si atoms is now replaced by a weaker bond associated to a delocalized molecular orbital, which also involves the original dangling-bond orbital.

We note that the energy diagram in Figure 7a representing the case of weak interaction also applies to the overlap between the dangling-bond orbital and the Si−X back-bond orbital with atoms X of high electronegativity. In this case, the energy level of the back-bond is well below that of the dangling bond, causing negligible spin transfer to the heteroatoms X. This is confirmed by the small values calculated for the spin densities ρ_X localized on heteroatoms X of high electronegativity, as compared to the spin densities ρ_B localized on the saturated Si neighbor (Table 3).

According to the described mechanism, the amount of spin transfer to the saturated Si atom depends on the relative energy levels of the dangling bond and the Si_A−Si_B back-bond. So far, we have seen that their relative energy levels can be modified by stabilizing the dangling-bond level through heteroatoms X of high electronegativity (Figure 7b). Another way of modifying their relative energy levels consists of destabilizing the back-bond by elongating the Si−Si bond length. As shown in the energy diagram in Figure 7c, such an elongation further enhances the spin transfer from the unsaturated to the saturated Si atom. Focusing on the model cluster with X = F, we illustrate in Figure 8 the behavior of the spin density difference $\rho_A - \rho_B$. As soon as the Si−Si bond length is larger than ∼2.85 Å, the spin density on the saturated Si atom exceeds that on the unsaturated one. In the limit of large Si−Si distances when the cluster breaks up into two components, the full spin localizes on the $\dot{S}i(SiH_3)_3$ unit, leaving the F_2Si component in a closed shell state ($^1A_1$). The observed behavior is not only limited to the case of fluorine heteroatoms but also occurs for the other model clusters. In particular, we also show in Figure 8 the evolution of the spin density difference for the cluster with X = Si. In this case, the energy difference between the interacting

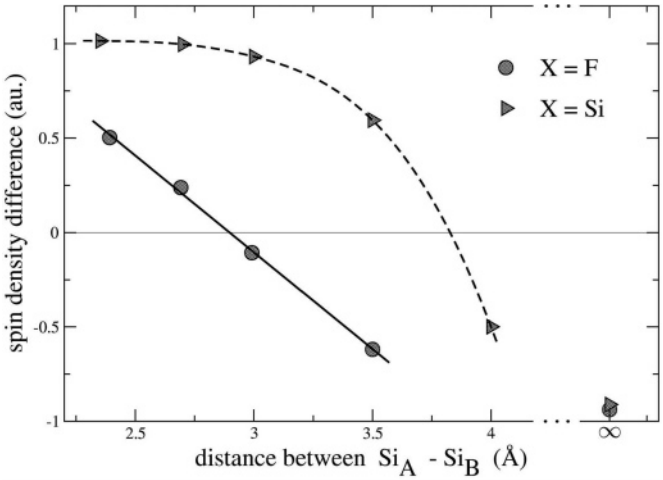

Figure 8. Difference between the spin densities localized on atoms Si_A and Si_B as a function of their bond length, for the clusters with X = F (disks) and X = Si (triangles). Only the Si_A-Si_B bond length is varied while all the other degrees of freedom are kept fixed at their original equilibrium values. The lines are guides to the eye.

orbitals is larger than in the cluster with X = F. However, a similar spin transfer is observed but corresponds to longer Si_A−Si_B bonds.

The present spin repulsion effect has experimentally been observed for the S center in thermal SiO_2 through an electron-spin-resonance signal involving two hyperfine interactions.[3] The comparison between experimental and theoretical hyperfine interactions favored the assignment to a central core containing a $\dot{S}i{\equiv}SiO_2$ unit embedded in the amorphous SiO_2 network.[1] The theoretical analysis revealed that the structural configurations in the amorphous environment could contain a higher degree of strain than in the idealized cluster models considered here, resulting in considerably longer Si−Si back-bonds. As illustrated in Figures 7c and 8, the weakening of the Si−Si back-bond amplifies the spin repulsion effect. Indeed, structural configurations modeling the $\dot{S}i{\equiv}SiO_2$ core unit in amorphous SiO_2 yielded an average contact interaction of 202 G for the saturated Si atom, more than a factor of 2 higher than found in the optimized clusters (77 G).[1] The amplification due to strain might favor the detectability of the hyperfine interactions of saturated Si atoms in the case of heteroatoms X with lower electronegativity than oxygen. For instance, we suggest that N-deficient amorphous Si_3N_4 is a good candidate material for showing a similar pair of hyperfine interactions.

The spin repulsion effect described above necessarily affects the reactivity of the radical silicon system. In fact, the delocalization of the dangling-bond orbital over the full cluster contributes to reducing the reactivity of the radical center in two ways. First, the center acquires a higher stability through the mechanism seen in Figure 7b. Second, the delocalization of the singly occupied molecular orbital reduces its exposure to external reactants. The smearing of the spin density over the Si−Si back-bond and the associated weakening of this bond (Table 2) should lead to an increase of the reactivity of the saturated Si atom. However, since this atom is sterically less accessible because of its fourfold coordination, the overall reactivity of the radical system is expected to diminuish. From the point of view of the reaction kinetics, this suggests a longer lifetime for Si radical centers when atoms of high electronegativity occur in the first-neighbor shell of the unsaturated Si atom.

It is interesting to contrast the electronic mechanism operating in the present spin repulsion effect with that governing hyperconjugation in organic chemistry. In general, hyperconjugation refers the delocalization of a σ bond leading to greater stability. Usually the σ electrons flow to empty orbitals, either p orbitals (e.g., as in carbocations) or to σ^*/π^* antibonding orbitals. When the hyperconjugation involves an unpaired electron, the interaction can occur either with filled or with empty orbitals.[17] The occurrence of hyperconjugation is usually associated with a substituent that directly participates with its interacting orbital in the delocalization. In other words, the hyperconjugative stabilization is driven by a delocalization that extends over the substituent atoms. For more details of the spin delocalization effect in organic free radicals, see refs. 18−20. The present spin repulsion effect shares some similarity with hyperconjugation as far as the stabilizing delocalization is concerned. However, in the spin repulsion effect, the delocalization does not involve the substituent (hetero) atoms. Instead, the delocalization takes place in the opposite direction, displacing the center of the spin farther away from the substituents: The spin is repelled from the unsaturated atom. The effect of the substituents is indirect: They affect the interaction between the dangling bond and the filled σ Si−Si bond by changing the hybrid state of the Si−X bond. It is important to note that this effect does not depend on the nature of the atoms bonded to the saturated Si atoms. Moreover, the same mechanism is operative when the unsaturated Si atom only binds to a single heteroatom, though the extent of the spin redistribution is smaller.[21]

Finally, we point out that the spin repulsion effect presented above may occur in a wider class of materials than Si-based radical centers. Indeed, we carried out test calculations on germanium-based radical clusters finding a similar large spin redistribution. This suggests that amorphous GeO_2 might also host a defect similar to the S center in amorphous SiO_2. On the other hand, we did not find such a spin delocalization in carbon analogues. There are a couple of factors that contribute to the marked difference between the Si or Ge radicals and their carbon analogues. First, the electronegativity difference between the carbon atom and the heteroatoms is not as large as for silicon, rendering the rehybridization effect weaker.[24] Furthermore, the smaller atomic radius of carbon gives rise to a larger repulsion between ligands, which results in a higher planarity around the unsaturated C atom.[25] Consequently, the dangling-bond orbital carries a higher degree of p character and increases its energy level, thereby reducing its interaction with the C−C bond and the corresponding spin delocalization. In fact, large spin redistributions as in silyl radicals have not been observed in C-based organic radicals.

We note that when the spin repulsion effect is absent, the neighboring saturated atom is found to carry a small spin density of *opposite* sign. We observe this peculiar effect in our calculations on silyl centers with X = Si, but also on C-based organic radicals. For instance, in the former case, we calculated a hyperfine contact interaction of $a_B = -3$ G on the saturated Si atom (cf. Table 3). Such a small and opposite contact interaction on a saturated neighbor has also been found in a theoretical investigation on Si dangling-bond defects at the Si(111)−SiO_2 interface.[23] We attribute this effect to a spin polarization effect by which the valence orbitals of the saturated atom are polarized by the unsaturated one. The majority spin is attracted toward the spin center, leaving excess minority spin on the saturated atom.[22] When the spin repulsion effect is operative, this tiny effect is masked.

Conclusions

In this work, we reveal a peculiar spin repulsion effect operative in silyl-radical systems containing atoms of high

electronegativity in the first-neighbor shell of the unsaturated Si atom. Calculations on cluster models containing main group atoms from either the first or second row show that a significant amount of spin density is transferred from the unsaturated Si to a neighboring saturated Si atom. The spin transfer is found to increase with the electronegativity of the heteroatoms.

The interaction of the unpaired orbital with the bonding Si−Si orbital is found to be at the origin of the spin repulsion effect. The electronegativity difference between the Si atoms and the heteroatoms X polarizes the Si−X bond, thereby increasing the degree of s character in the dangling-bond orbital. By consequence, the energy level of the dangling bond shifts downward, increasing its interaction with the Si−Si back-bond. This mechanism successfully explains all the trends in the structural, electronic, and hyperfine properties calculated for varying electronegativities of the heteroatoms.

The mechanism is general and can operate in both the gas and solid phases. The described delocalization of the spin density has been used to assign the S center in amorphous SiO_2. Our work suggests that amorphous Si_3N_4 and GeO_2 are other materials that present favorable conditions for the experimental observation of this effect.

Note Added after ASAP Publication. This article was released ASAP on August 27, 2005. In the Results and Discussion section, paragraph 7, sentence 1 has been revised. In the Conclusions section, paragraph 1, sentence 1 has been revised. The correct version was posted on August 30, 2005.

References and Notes

(1) Stirling, A.; Pasquarello, A. *Phys. Rev. B* **2002**, *66*, 245201.

(2) Stirling, A.; Pasquarello, A.; Charlier, J.-C.; Car, R. *Phys. Rev. Lett.* **2000**, *85*, 2773−2776. Stirling, A.; Pasquarello, A.; Charlier, J.-C.; Car, R. In *Physics and Chemistry of SiO_2 and the Si−SiO_2 Interface-4*; Massoud, H. Z., Baumvol, I. J. R., Hirose, M., Poindexter, E. H., Eds.; The Electrochemical Society: Pennington, 2000; pp 283−289.

(3) Stesmans, A.; Nouwen, B.; Afanas'ev, V. V. *Appl. Phys. Lett.* **2002**, *80*, 4753.

(4) (a) Becke, A. D. *J. Chem. Phys.* **1993**, *98*, 5648−5652. (b) Lee, C. T.; Yang, W. T.; Parr, R. G. *Phys. Rev. B* **1988**, *37*, 785−789.

(5) Barone, V. In *Recent Advances in Density Functional Methods, Part I*; Chong, D. P. Ed.; World Scientific Publishing Co.: Singapore, 1996; pp 287−334.

(6) Kutzelnigg, W.; Fleischer, U.; Schindler, I. M. *The IGLO-Method: Ab Initio Calculation and Interpretation of NMR Chemical Shifts and Magnetic Susceptibilities*; Springer- Verlag: Heidelberg, 1990; Vol. 23.

(7) Basis sets were obtained from the Extensible Computational Chemistry Environment Basis Set Database, version 02/25/04, as developed and distributed by the Molecular Science Computing Facility, Environmental and Molecular Sciences Laboratory, which is part of the Pacific Northwest Laboratory, P.O. Box 999, Richland, WA 99352, U.S.A., and funded by the U.S. Department of Energy. The Pacific Northwest Laboratory is a multiprogram laboratory operated by Battelle Memorial Institute for the U.S. Department of Energy under contract DE-AC06-76RLO 1830. Contact David Feller or Karen Schuchardt for further information.

(8) (a) Frisch, M. J.; Trucks, G. W.; Schlegel, H. B.; Scuseria, G. E.; Robb, M. A.; Cheeseman, J. R.; Zakrzewski, V. G.; Montgomery, J. A., Jr.; Stratmann, R. E.; Burant, J. C.; Dapprich, S.; Millam, J. M.; Daniels, A. D.; Kudin, K. N.; Strain, M. C.; Farkas, O.; Tomasi, J.; Barone, V.; Cossi, M.; Cammi, R.; Mennucci, B.; Pomelli, C.; Adamo, C.; Clifford, S.; Ochterski, J.; Petersson, G. A.; Ayala, P. Y.; Cui, Q.; Morokuma, K.; Malick, D. K.; Rabuck, A. D.; Raghavachari, K.; Foresman, J. B.; Cioslowski, J.; Ortiz, J. V.; Stefanov, B. B.; Liu, G.; Liashenko, A.; Piskorz, P.; Komaromi, I.; Gomperts, R.; Martin, R. L.; Fox, D. J.; Keith, T.; Al-Laham, M. A.; Peng, C. Y.; Nanayakkara, A.; Gonzalez, C.; Challacombe, M.; Gill, P. M. W.; Johnson, B. G.; Chen, W.; Wong, M. W.; Andres, J. L.; Head-Gordon, M.; Replogle, E. S.; Pople, J. A. *Gaussian 98*, revision A.11; Gaussian, Inc.: Pittsburgh, PA, 1998. (b) Frisch, M. J.; Trucks, G. W.; Schlegel, H. B.; Scuseria, G. E.; Robb, M. A.; Cheeseman, J. R.; Montgomery, J. A., Jr.; Vreven, T.; Kudin, K. N.; Burant, J. C.; Millam, J. M.; Iyengar, S. S.; Tomasi, J.; Barone, V.; Mennucci, B.; Cossi, M.; Scalmani, G.; Rega, N.; Petersson, G. A.; Nakatsuji, H.; Hada, M.; Ehara, M.; Toyota, K.; Fukuda, R.; Hasegawa, J.; Ishida, M.; Nakajima, T.; Honda, Y.; Kitao, O.; Nakai, H.; Klene, M.; Li, X.; Knox, J. E.; Hratchian, H. P.; Cross, J. B.; Bakken, V.; Adamo, C.; Jaramillo, J.; Gomperts, R.; Stratmann, R. E.; Yazyev, O.; Austin, A. J.; Cammi, R.; Pomelli, C.; Ochterski, J. W.; Ayala, P. Y.; Morokuma, K.; Voth, G. A.; Salvador, P.; Dannenberg, J. J.; Zakrzewski, V. G.; Dapprich, S.; Daniels, A. D.; Strain, M. C.; Farkas, O.; Malick, D. K.; Rabuck, A. D.; Raghavachari, K.; Foresman, J. B.; Ortiz, J. V.; Cui, Q.; Baboul, A. G.; Clifford, S.; Cioslowski, J.; Stefanov, B. B.; Liu, G.; Liashenko, A.; Piskorz, P.; Komaromi, I.; Martin, R. L.; Fox, D. J.; Keith, T.; Al-Laham, M. A.; Peng, C. Y.; Nanayakkara, A.; Challacombe, M.; Gill, P. M. W.; Johnson, B.; Chen, W.; Wong, M. W.; Gonzalez, C.; Pople, J. A. *Gaussian 03*, revision C.01; Gaussian, Inc.: Wallingford, CT, 2004.

(9) Gavartin, J. L.; Sushko, P. V.; Shluger, A. L. *Phys. Rev. B* **2003**, *67*, 035108.

(10) Pacchioni, G.; Frigoli, F.; Ricci, D. *Phys. Rev. B* **2000**, *63*, 054102.

(11) Lægsgaard, J.; Stokbro, K. *Phys. Rev. Lett.* **2001**, *it 86*, 2834.

(12) Bent, H. A. *Chem. Rev.* **1961**, *61*, 275−311.

(13) Cherry, W.; Epiotis, N.; Borden, W. T. *Acc. Chem. Res.* **1977**, *10*, 167−173.

(14) Guerra, M. *J. Am. Chem. Soc.* **1993**, *115*, 11926−11929.

(15) Houk, K. N. *Acc. Chem. Res.* **1975**, *8*, 361−369.

(16) Chatgilialoglu, C. *Chem. Rev.* **1995**, *95*, 1229−1251.

(17) Viehe, H. G.; Janousek, Z.; Merényi, R.; Stella, L. *Acc. Chem. Res.* **1985**, *18*, 148−154.

(18) Nonhebel, D. C.; Walton, J. C. *Free Radical Chemistry*; Cambridge University Press: London, 1974.

(19) King, F. W. *Chem. Rev.* **1976**, *76*, 157−186.

(20) Improta, R.; Barone, V. *Chem. Rev.* **2004**, *104*, 1231−1253.

(21) Unpublished results.

(22) Morton, J. R. *Chem. Rev.* **1964**, *64*, 453−471.

(23) Similar spin-polarization effect was observed in solid state: Cook, M.; White, C. T. *Phys. Rev. B* **1988**, *38*, 9674−9685.

(24) Guerra, M. *J. Phys. Chem.* **1995**, *99*, 81−84.

(25) Pacansky, J.; Koch, W.; Miller, M. D. *J. Am. Chem. Soc.* **1991**, *113*, 317−328.